THE JOURNAL OF PHYSICAL CHEMISTRY A LETTERS

2006, *110,* 5978−5981
Published on Web 04/18/2006

Time-Dependent Wave Packet Studies on the Cl + HCl Hydrogen Exchange Reaction

Gé W. M. Vissers and Anne B. McCoy*

Department of Chemistry, The Ohio State University, Columbus, Ohio 43210

Received: February 24, 2006; In Final Form: March 23, 2006

The initiation of the hydrogen exchange reaction $Cl(^2P) + HCl \rightarrow ClH + Cl(^2P)$ by excitation of the HCl molecular stretch to $v = 2$ is studied for total angular momentum quantum number $J = {}^1/_2$ and both even and odd parity. The calculations were performed using a time-dependent propagation from an initial quasi-bound state and employed all three relevant potential energy surfaces and the nonadiabatic couplings between them. Coriolis and spin−orbit coupling were also taken into account. The electronic and HCl rotational distributions of the products in both dissociation channels are analyzed, and the results are interpreted using features of the potential energy surfaces.

1. Introduction

In recent years, interest in reactions in which open-shell species play a role is increasing. On the experimental side, spectroscopic studies are being combined with theory to study van der Waals complexes of hydride radicals with rare gas atoms[1−7] and molecular hydrogen.[8,9] Also, larger hydrogen-bonded reactant complexes containing the OH radical, like OH−CO,[10−14] OH−N_2,[15] OH−H_2O,[16] and OH−C_2H_2,[17,18] which are of interest in atmospheric and combustion processes, have been studied with spectroscopy and model calculations. Much of the experimental work on these molecular complexes was motivated by two factors. First, they enable researchers to probe prereactive complexes and their role in chemical reaction dynamics. In addition, these studies have been used to investigate the possibility of initiating reactions through vibrational excitation of a high-frequency mode of one of the molecules in the complex. Here, the idea is that if one can give the system just enough energy to overcome the barrier for reaction, the product state distributions should provide insights into the potential energy surface.

On the theoretical side, the most common approach for describing chemical reactions is to assume that they take place within a single electronic state, so that the atoms move on a single adiabatic potential energy surface (PES). In reactions where one of the reactant molecules is an open-shell species, multiple coupled potential energy surfaces must be considered to obtain an accurate model of the reaction dynamics.

Reactions between hydrogen halide molecules and halogen atoms form an important prototype in the study of the reactions involving open-shell species. Due to their relative simplicity, they can be studied in great detail. One such reaction which has received much attention over the years is the hydrogen exchange reaction $Cl(^2P) + HCl \rightarrow ClH + Cl(^2P)$. In this reaction, there are three electronic surfaces that correlate to the ground state of the reactants and products. Multiple electronic structure studies have been devoted to describing these surfaces, in the van der Waals well only[19] as well as globally.[20−22] The dynamics of the system has been studied in a variety of ways, including calculations of van der Waals bound states[23−26] and quantum scattering calculations.[20,27−30]

In this letter, we report results of a time-dependent wave packet study in which we investigate the feasibility of initiating the hydrogen exchange reaction in $Cl(^2P) + HCl$ by vibrational excitation of the HCl molecule. Time-dependent wave packet propagation has been used before in the study of other electronically nonadiabatic systems such as Cl + H_2,[31] B + H_2,[32] and O + N_2[33] scattering and reactions of $H^+ + H_2$,[34,35] F + H_2,[36−39] and O+ H_2.[40] A schematic overview of the Cl + HCl reaction process is given in Figure 1. The primary goals of this work are to determine if vibrational excitation of the HCl can initiate this hydride transfer reactions as well as to investigate which effects are important in determining the branching ratio between vibrational predissociation and reaction. We also investigate the role of the multiple potential surfaces on the reaction dynamics.

The calculations start from a quasi-bound van der Waals complex, in which the HCl molecule is excited to its first overtone. The evolution of the wave packet in time is computed using a Chebyshev propagator. We calculate the branching ratio between direct dissociation, in which the system falls apart in the original Cl atom and HCl molecule, and reaction, where the hydrogen atom is transferred from one Cl atom to the other. Furthermore, we analyze the resulting products in terms of their electronic and rotational distributions.

2. Theory

The Cl + HCl system is described in a body-fixed (BF) frame in which the *z*-axis is chosen to correspond to the vector **R** that connects the Cl atom to the center of mass of the HCl molecule. The BF frame is related to a laboratory frame by a rotation over angles (β, α), which are the polar angles of **R** with respect to the space-fixed frame. The orientation of the HCl molecule in the BF frame is defined by the polar angles (θ, ϕ), where θ is the angle between **R** and the HCl bond vector **r** and ϕ is an azimuthal angle. The linear Cl−HCl geometry corresponds to $\theta = 0$.

10.1021/jp061196d CCC: $33.50

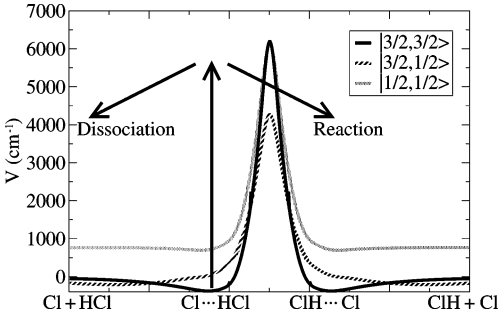

Figure 1. Schematic overview of the reaction process. The surfaces correspond to the diagonal components of the diabatic potentials which have been minimized with respect to θ. The barrier heights are 4262, 6129, and 6187 cm^{-1}, while the initially prepared state has an energy of 5608 cm^{-1}.

The diabatic potentials that are used in the calculations are the ab initio potentials computed by Dobbyn et al.,[22] with scaled barrier heights as described in ref 28. The matrix elements of these potentials in a basis of electronic orbital angular momentum functions $|l, \lambda\rangle$ were reexpanded in the form

$$V_{\lambda'\lambda}(R, r, \theta, \phi) = \langle l\lambda'|\hat{V}|l\lambda\rangle = \sum_{l_b} v_{l_b}^{\lambda'\lambda}(R, r) C_{l_b,\lambda'-\lambda}(\theta, \phi) \quad (1)$$

Here, $l = 1$ is the total electronic orbital angular momentum quantum number of the Cl atom, and λ', $\lambda = -1, 0, 1$ are projections of the electronic orbital angular momentum on **R**. The functions $C_{l_b,\lambda'-\lambda}(\theta, \phi)$ are spherical harmonics in Racah normalization. The expansion was carried out on evenly spaced grids in R and r, using 130 points in the range 3.5−12 a_0 for R and 75 points between 1.0 and 4.5 a_0 for r, and was taken up to $l_b = 12$.

The complex is described in a parity-adapted basis consisting of direct products of radial and angular functions. For the angular part, an uncoupled two-angle embedded BF basis

$$|\gamma j_a \omega_a j_b \omega_b \Omega\rangle = |j_a \omega_a\rangle^{\gamma} Y_{j_b\omega_b}(\theta_\gamma, \phi_\gamma)\left[\frac{2J+1}{4\pi}\right]^{1/2} D^{J*}_{M\Omega}(\alpha_\gamma, \beta_\gamma, 0) \quad (2)$$

was used. The spherical harmonics $Y_{j_b\omega_b}(\theta_\gamma, \phi_\gamma)$ describe the rotation of the HCl molecule with respect to the dimer fixed frame, while the Wigner rotation functions $D^{J*}_{M\Omega}(\alpha_\gamma, \beta_\gamma, 0)$ describe the rotation of the complex as a whole. The label $\gamma = r, p$ refers to the arrangement channel of the complex: for $\gamma = r$, the angles and distances are the Jacobi coordinates for the reactant complex Cl_a-HCl_b; if $\gamma = p$, they describe the system in coordinates suited to the product complex Cl_aH-Cl_b. The kets $|j_a, \omega_a\rangle$ are used to describe the electronic angular momentum of the Cl atom and are a coupled product of spin and orbital angular momentum functions

$$|j_a, \omega_a\rangle^{\gamma} = \sum_{\lambda\sigma} |l\lambda\rangle^{\gamma} |s\sigma\rangle^{\gamma} \langle l\lambda s\sigma | j_a \omega_a\rangle \quad (3)$$

The spin−orbit coupling $A\hat{\mathbf{l}}\cdot\hat{\mathbf{s}} = A(\hat{j}_a^2 - \hat{l}^2 - \hat{s}^2)/2$ is diagonal in this basis. The diabatic potential surfaces are the matrix elements of $\hat{V} + A\hat{\mathbf{l}}\cdot\hat{\mathbf{s}}$ in this atomic basis. The adiabatic potentials are obtained by diagonalization of this matrix. Rotational functions up to $j_b = 12$ were used. The angular basis is restricted by the relation $\Omega = \omega_a + \omega_b$.

The radial basis functions are obtained by a two-dimensional sinc function discrete variable representation,[41] using the lowest adiabatic potential on the same radial grid as was used in the expansion of the potential surfaces. A total of 90 radial functions were used in the calculations in both arrangement channels. These are the 10 lowest stretch functions for the monomer stretch ground state, combined with 20 radial functions centered in energy around the first 4 monomer stretch excited states.

The spin−orbit coupling constant A was kept fixed at its atomic value of −588.27 cm^{-1}. The masses used in the calculations were 1.0 078 250 u for H, 34.9 688 527 u for ^{35}Cl, and 36.9 659 026 u for ^{37}Cl. All calculations were performed for total angular momentum quantum number $J = {}^1/_2$.

The initial state for the reaction was calculated as a quasi-bound state using only the reactant arrangement channel. This wave packet was then propagated in time up to 4.8 ns using a Chebyshev propagator with a time step of 100 au (2.42 fs). In each time step, the part of the wave packet where the separation between the atom and the molecule was greater than 9.0 a_0 was damped with a Gaussian function with a width of 2.0 a_0. All calculations presented here started from the second monomer stretch excited state of the complex, which has a vibrational energy of 5608.02 cm^{-1}.

3. Results and Discussion

Analysis of the wave packet shows that vibrational excitation of the HCl molecule initiates the hydrogen exchange reaction. In Figure 2a, the distribution of the wave packet density over the reactant and product channels is plotted. The initial buildup of density in the product channel is relatively fast (∼100 ps). After this period, the wave packet starts oscillating back and forth between the reactant and product channels as it dissociates. Integration of the wave packet over time shows that approximately 43% of the dissociation products has undergone hydrogen exchange.

In Figure 2b, the total density in the bound region ($R < 9$ a_0) is plotted as a function of time, for the three initial isotopologues $^{35}Cl-H^{35}Cl$, $^{37}Cl-H^{35}Cl$, and $^{35}Cl-H^{37}Cl$. The effect of starting with an isotopically substituted Cl−HCl complex is very minor. The density was fit to a biexponential decay function

$$D(t) = \alpha_1 \exp(-t/\tau_1) + \alpha_2 \exp(-t/\tau_2) + 1 - \alpha_1 - \alpha_2$$

The parameters of this fit are given in Table 1 for $^{35}Cl-H^{35}Cl$. The parameters for the other two isotopologues differ by less than 10% from those reported in Table 1. As can be seen in Table 1, the effect of parity on the total decay time is very small. While the symmetry of the Cl + HCl reaction makes the nearly equal branching for dissociation and reaction not very surprising, the relative insensitivity of the reaction rates, branching, and as we will see, product state distribution when one of the chlorine atoms is replaced with ^{37}Cl is surprising.

The dissociation products were analyzed by integrating the dissociated parts of the wave packet (the parts removed by the damping procedure) over time. In Table 1, the distribution of the wave packet over the three diabatic potential energy surfaces is given. It shows that the part of the wave packet that dissociates in the product channel has a slightly higher preference for the $|j_a, |\omega_a|\rangle = |{}^3/_2, {}^1/_2\rangle$ surface than the part that dissociates directly. A possible explanation for this observation may be found in Figure 1, which shows that, on top of the reaction barrier, the surface is much lower in energy than the $|{}^3/_2, {}^3/_2\rangle$ PES. In fact, only the barrier on the $|{}^3/_2, {}^1/_2\rangle$ state is lower than the energy that is put into the system by exciting the first overtone of the HCl stretch. Note that, for both dissociation channels, the contribution of the $|{}^3/_2, {}^1/_2\rangle$ and $|{}^1/_2, {}^1/_2\rangle$ surfaces in the products

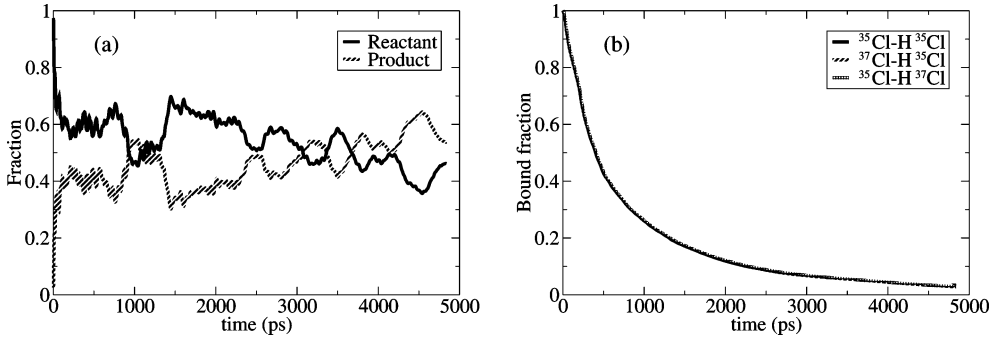

Figure 2. (a) Distribution of the wave packet over the dissociation channels. The distribution is normalized with respect to the total amount of the wave packet with Cl−HCl distances of $< 9\ a_0$. (b) Total density of the wave packet in the bound region. The differences between the three isotopologues are too small to be noticed.

TABLE 1: Biexponential Fit Parameters and Electronic Product State Distributions for ^{35}Cl−H^{35}Cl

Fit Parameters		
	e parity	*f* parity
α_1	0.573	0.564
τ_1 (ps)	354	358
α_2	0.403	0.422
τ_2 (ps)	1381	1418

Electronic Distributions				
	react.	prod.	react.	prod.
$\|^3/_2, {}^3/_2\rangle$	41.0%	31.3%	38.5%	29.2%
$\|^3/_2, {}^1/_2\rangle$	54.4%	63.6%	51.8%	60.4%
$\|^1/_2, {}^1/_2\rangle$	4.5%	5.0%	9.6%	10.4%

is larger than it is in the original wave packet, which had 69% of its probability amplitude in the $|^3/_2, {}^3/_2\rangle$ state and 30% $|^3/_2, {}^1/_2\rangle$. The dissociation products from the states of *f* symmetry show a higher contribution of the $|^1/_2, {}^1/_2\rangle$ surface than the products of *e* parity, both in the reactant channel and in the product channel. Since the electronic distributions for the initial states of both parities are nearly equal, it is in the dissociation process itself that the parity of the wave function is important. This change in branching for the different electronic states hints at the fact that nonadiabatic effects are playing a role in the dynamics of these photoinitiated reactions.

The HCl rotational distribution for the ^{35}Cl−H^{35}Cl system of *e* parity is plotted in Figure 3. The rotational distributions for the other isotopologues and parity look very similar. If we divide the distribution by electronic states, the distributions for the $|^3/_2, {}^1/_2\rangle$ and the $|^3/_2, {}^3/_2\rangle$ states are nearly identical for the dissociating part, while for the reacting part, the $|^3/_2, {}^1/_2\rangle$ distribution is colder than the $|^3/_2, {}^3/_2\rangle$ one. Comparing the dissociating and reacting parts of the wave packet, we find that the directly dissociating part of the wave packet comes out ∼100 cm^{-1} rotationally warmer than the reacting part. These observations can be rationalized by the fact that, in the case of reaction, it is anticipated that a larger fraction of the energy will go into translation, as that motion most closely correlates with the initial HCl vibrational excitation. As a result, less energy ends up in rotation. The difference between the rotational distributions for the two electronic states for the reacting part is attributed to the dependence of the coupling between these states on j_b.

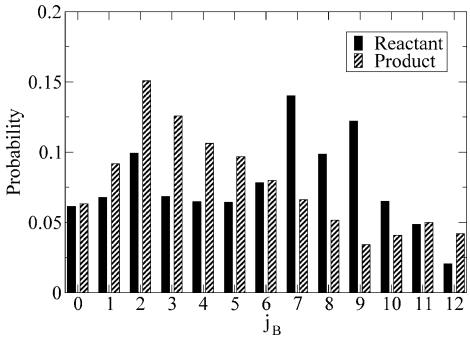

Figure 3. HCl rotational product state distribution for dissociation from ^{35}Cl−H^{35}Cl of *e* parity.

4. Conclusion

Our time-dependent wave packet calculations show that it is possible to make the Cl(^2P) + HCl system react by vibrationally exciting the HCl molecule. The effect of substitution of either of the Cl atoms by ^{37}Cl on the reaction is very small, and the product state distributions are affected only slightly. We observe a change in rotational and electronic product state distributions for the products after reaction as compared to direct dissociation.

Acknowledgment. Support for this work from the Chemistry Division of the National Science Foundation is gratefully acknowledged. We thank Professors Marsha Lester and Michael Heaven for many discussions on these processes. We also thank Professor George Schatz for providing us with the potential routines used in this work.

References and Notes

(1) Komissarov, A. V.; Heaven, M. C. *J. Chem. Phys.* **2000**, *113*, 1775.
(2) Bonn, R. T.; Wheeler, M. D.; Lester, M. I. *J. Chem. Phys.* **2000**, *112*, 4942.
(3) Kerenskaya, G.; Schnupf, U.; Heaven, M. C.; van der Avoird, A. *J. Chem. Phys.* **2004**, *121*, 7549.
(4) Kerenskaya, G.; Schnupf, U.; Heaven, M. C.; van der Avoird, A.; Groenenboom, G. C. *Phys. Chem. Chem. Phys.* **2005**, *7*, 846.
(5) Kerenskaya, G.; Schnupf, U.; Basinger, W. H.; Heaven, M. C. *J. Chem. Phys.* **2005**, *123*, 054304.
(6) Han, J.; Heaven, M. C. *J. Chem. Phys.* **2005**, *123*, 064307.
(7) Heaven, M. C. *Int. Rev. Phys. Chem.* **2005**, *24*, 375.
(8) Wheeler, M. D.; Anderson, D. T.; Lester, M. I. *Int. Rev. Phys. Chem.* **2000**, *19*, 501.
(9) Fawzy, W. M.; Kerenskaya, G.; Heaven, M. C. *J. Chem. Phys.* **2005**, *122*, 144318.
(10) Lester, M. I.; Pond, B. V.; Anderson, D. T.; Harding, L. B.; Wagner, A. F. *J. Chem. Phys.* **2000**, *113*, 9889.
(11) Lester, M. I.; Pond, B. V.; Marshall, M. D.; Anderson, D. T.; Harding, L. B.; Wagner, A. F. *Faraday Discuss.* **2001**, *118*, 373.
(12) Pond, B. V.; Lester, M. I. *J. Chem. Phys.* **2003**, *118*, 2223.
(13) Pollack, I. B.; Tsiouris, M.; Leung, H. O.; Lester, M. I. *J. Chem. Phys.* **2003**, *119*, 118.
(14) Marshall, M. D.; Pond, B. V.; Lester, M. I. *J. Chem. Phys.* **2003**, *118*, 1196.
(15) Marshall, M. D.; Pond, B. V.; Hopman, S. M.; Lester, M. I. *J. Chem. Phys.* **2001**, *114*, 7001.
(16) Marshall, M. D.; Lester, M. I. *J. Phys. Chem. B* **2005**, *109*, 8400.
(17) Davey, J. B.; Greenslade, M. E.; Marshall, M. D.; Lester, M. I. *J. Chem. Phys.* **2004**, *121*, 3009.
(18) Marshall, M. D.; Davey, J. B.; Greenslade, M. E.; Lester, M. I. *J. Chem. Phys.* **2004**, *121*, 5845.

(19) Kłos, J. A.; Chałasiński, G.; Szczęśniak, M. M.; Werner, H.-J. *J. Chem. Phys.* **2001**, *115*, 3085.
(20) Maierle, C. S.; Schatz, G. C.; Gordon, M. S.; McCabe, P.; Connor, J. N. L. *J. Chem. Soc., Faraday Trans.* **1997**, *93*, 709.
(21) González, M.; Hijazo, J.; Novoa, J. J.; Sayós, R. *J. Chem. Phys.* **1998**, *108*, 3168.
(22) Dobbyn, A. J.; Connor, J. N. L.; Besley, N. A.; Knowles, P. J.; Schatz, G. C. *Phys. Chem. Chem. Phys.* **1999**, *1*, 957.
(23) Dubernet, M.-L.; Hutson, J. M. *J. Phys. Chem.* **1994**, *98*, 5844.
(24) Žďánska, P.; Nachtigallová, D.; Nachtigall, P.; Jungwirth, P. *J. Chem. Phys.* **2001**, *115*, 5974.
(25) Zeimen, W. B.; Klos, J. A.; Groenenboom, G. C.; van der Avoird, A. *J. Phys. Chem. A* **2003**, *107*, 5110.
(26) Zeimen, W. B.; Klos, J. A.; Groenenboom, G. C.; van der Avoird, A. *J. Phys. Chem. A* **2004**, *108*, 9319.
(27) Schatz, G. C.; McCabe, P.; Connor, J. N. L. *Faraday Discuss.* **1998**, *110*, 139.
(28) Whiteley, T. W. J.; Dobbyn, A. J.; Connor, J. N. L.; Schatz, G. C. *Phys. Chem. Chem. Phys.* **2000**, *2*, 549.
(29) Schatz, G. C.; Hankel, M.; Whiteley, T. W. J.; Connor, J. N. L. *J. Phys. Chem. A* **2003**, *107*, 7278.
(30) Hankel, M.; Connor, J. N. L.; Schatz, G. C. *Chem. Phys.* **2005**, *308*, 225.
(31) Ghosal, S.; Mahapatra, S. *J. Phys. Chem. A* **2005**, *109*, 1530.
(32) Yang, S. H.; Weeks, D. E.; Niday, T. A. *Chem. Phys. Lett.* **2005**, *410*, 316.
(33) Chu, T.-S.; Xie, T.-X.; Han, K.-L. *J. Chem. Phys* **2004**, *121*, 9352.
(34) Chu, T.-S.; Han, K.-L. *J. Phys. Chem. A* **2005**, *109*, 2050.
(35) Lu, R.-F.; Chu, T.-S.; Han, K.-L. *J. Phys. Chem. A* **2005**, *109*, 6683.
(36) Xie, T.-X.; Zhang, Y.; Zhao, M.-Y.; Han, K.-L. *Phys. Chem. Chem. Phys.* **2003**, *5*, 2034.
(37) Zhang, Y.; Xie, T.-X.; Han, K.-L. *J. Phys. Chem. A* **2003**, *107*, 10893.
(38) Zhang, Y.; Xie, T.-Z.; Han, K.-L.; Zhang, J. Z. H. *J. Chem. Phys.* **2003**, *119*, 12921.
(39) Zhang, Y.; Xie, T.-X.; Han, K.-L.; Zhang, J. Z. H. *J. Chem. Phys.* **2004**, *120*, 6000.
(40) Chu, T.-S.; Zhang, X.; Han, K.-L. *J. Chem. Phys.* **2005**, *122*, 214301.
(41) Colbert, D. T.; Miller, W. H. *J. Chem. Phys.* **1992**, *96*, 1982.